Available online at www.sciencedirect.com
SCIENCE DIRECT®
Chemical Physics Letters 370 (2003) 451–459
CHEMICAL PHYSICS LETTERS
www.elsevier.com/locate/cplett

Ab initio calculations of equilibrium geometries and vibrational excitations of helical ethylene-glycol oligomers: application to modeling of monolayer infrared spectra

Lyuba Malysheva [a], Yuriy Klymenko [b], Alexander Onipko [c], Ramūnas Valiokas [d], Bo Liedberg [d,*]

[a] *Bogolyubov Institute for Theoretical Physics, Kiev, 03143, Ukraine*
[b] *Space Research Institute, Kiev, 03187, Ukraine*
[c] *Division of Physics, Luleå University of Technology, S-971 87 Luleå, Sweden*
[d] *Division of Sensor Science and Molecular Physics, Department of Physics and Measurement Technology, Linköping University, S-581 83 Linköping, Sweden*

Received 7 November 2002; in final form 13 January 2003

Abstract

The density functional theory methods are used to calculate the equilibrium molecular structures and vibrational spectra of helical $H(CH_2CH_2O)_nH$ (OEG) oligomers ($n = 4$–7) at a level of precision that has not been accomplished before. The largest deviation between experimentally observed frequencies, obtained from infrared reflection–absorption spectra of OEG-monolayers on gold, and calculated, single molecule frequencies (unscaled), is slightly above 2%. Moreover, the most intense peak in the CH_2-stretching region at about 2890 cm^{-1}, commonly regarded as a trademark of the OEG helical conformation, is reassigned in this study to the asymmetric CH_2-stretching mode.

1. Introduction

During the last decade, different kinds of self-assembled monolayers (SAMs) have received considerable research attention as templates for the development of novel organic materials [1–4], electronic device-oriented structures [5], biomolecular recognition devices and sensors [6], as well as in a variety of other fundamental and applied contexts. From the point of view of new biomaterials, for example, a substantial amount of research effort has been focused on studies aimed at finding correlations between the conformational/wetting and the protein repellent properties of oligo-(ethylene glycol) (OEG)-terminated SAMs.

The assembly properties of OEG-terminated alkanethiolates on gold were for the first time studied by Pale-Grosdemange et al. [7]. The conformational

* Corresponding author. Fax: +46-0-13-288969.
E-mail address: bolie@ifm.liu.se (B. Liedberg).

0009-2614/03/$ - see front matter
doi:10.1016/S0009-2614(03)00116-7

properties of the OEG-SAMs were later investigated in detail, on different supporting lattices, by Grunze and co-workers [8,9], and they reported on the existence of two stable conformers – a helical on gold and an all *trans* on silver. Vanderah et al. [10] developed a series of structurally well-defined, but reversed, OEG-SAMs on gold, where the SH group was attached to the OEG terminus rather than to the alkyl terminus i.e., $HS(CH_2CH_2O)_6R$, where R is an *n*-alkyl group of length 10 or 18. The helical OEG-SAMs were also found to undergo a reversible temperature-driven conformational transition from the helical to the all-*trans* state at about 60 °C [11].

The accomplished understanding of the above properties is largely based on infrared reflection–absorption (RA) spectroscopy measurements. According to the surface selection rule valid for SAMs supported by reflective metallic substrates, the infrared absorption of an arbitrary vibrational mode is determined by the projection of its transition dipole moment (TDM) on the normal to the surface. Consequently, the apparent intensity distribution in the spectrum is strongly dependent on the molecular orientation within the SAM. Thus, a detailed analysis of the peak intensities enables one to draw far-reaching conclusions about the orientation of alkyl and OEG chains relative to the substrate surface, provided that the corresponding TDMs (in molecular coordinates) are known, and this specific feature of RA spectroscopy will be utilized in this work. It should at this point be emphasized that the assignments and TDMs of the main features in the infrared spectra of OEGs are fairly well understood primarily because of the extensive theoretical and experimental investigations by Miyazawa et al. [12a,12b,12c], where the helical conformation of ethylene glycols was established on the basis of the standard normal-coordinate treatment of an infinitely long molecule. The authors also calculated the frequencies of normal vibrations by using the GF-matrix method [13]. The assignments of the main peaks were justified by comparing the observed spectra with those of short related molecules [12a,12b,14]. The results of these analyses have been extensively used for the identification of the OEG contribution to RA spectra of OEG-containing SAMs [8–11] (and references therein).

The ever-increasing interest to the family of ethylene-glycol oligomers for various technological and surface chemical/biological applications also has stimulated theoreticians to perform extensive studies on relatively small model compounds using ab initio methods. To mention a few, HF calculations of the optimized geometry of diglyme ($H_3C(OCH_2CH_2)_2OCH_3$) and its conformers were performed by Gejji et al. [15]. The conformational energies of the DME molecule ($H_3COCH_2CH_2OCH_3$) and its vibrational frequencies, in the fingerprint region, were reported at the HF level by Jaffee et al. [16]. The energies of different conformations of OEG molecules (of the type $(OCH_2CH_2)_n$–OMe, $n = 1$–4) and their interaction with water were investigated in detail by Wang et al. [17] on the basis of the DFT methods. That study confirmed that the helical conformer of OEG has the lowest energy comparing with other possible OEG conformers.

The ab initio results reported so far refer exclusively to the structure and/or vibrational frequencies of relatively simple OEG-containing compounds. To the best of our knowledge, first-principle modeling of the infrared spectra, which admits a straightforward comparison with measured spectra, has not been attempted before. This Letter presents, for the first time, a comparison between simulated spectra obtained with the use of the DFT-LSDA method and RA spectra of OEG-terminated SAMs on gold [11]. We concentrate on the helical OEG conformer (i.e., on the OEG units with *gauche* O–C–C–O and *trans* C–O–C–C angles) which according to a gross number of theoretical and experimental data dominates the OEG-SAMs in focus [8–11,17]. The assignments of Miyazawa, which were never tested at the ab initio level, are revised and corrected.

2. Methodology

2.1. Computational details

The helical-like optimized geometry of ethylene-glycol oligomers was obtained by the DFT-LSDA

and HF methods with 3-21G* and 6-31G** basis sets as suggested by the GAUSSIAN 98 package of programs. The accuracy cross-check was provided by the use of the MP2 method and the DFT method with the B3LYP exchange-correlation functional. All these methods were then tried in calculations of OEG vibrational spectra. The final choice of the method most suitable for our modeling has been guided by the comparison with the data available from the literature and experiment, as shown below.

2.2. Infrared reflection–absorption spectroscopy

The RA spectra were recorded on a Bruker IFS66 Fourier transform spectrometer equipped with a grazing angle of incidence reflection accessory aligned at 85° and a wire grid polarizer (p-polarized). A liquid nitrogen cooled MCT detector was used. Interferograms were apodized with a three-term Blackmann–Harris function before Fourier transformation. The spectra were recorded by averaging 3000 interferograms (10 min) at 2 cm^{-1} resolution.

2.3. Sample preparation and chemicals

The supporting substrates were standard (1 0 0) Si wafers cut to appropriate sizes and coated with 25 Å titanium followed by 2000 Å gold using an electron-beam evaporation system. Further details about the gold deposition procedure can be found elsewhere [11]. The gold surfaces were cleaned before the thiol adsorption in a 5:1:1 mixture of de-ionized MilliQ water, 25% hydrogen peroxide and 30% ammonia at 80 °C for 5 min. The procedure was repeated until the optical parameters measured by an automatic Rudolph Research AutoEl ellipsometer (He–Ne laser light source $\lambda = 632.8$ nm, angle of incidence 70°) indicated a clean gold surface, free from organic contamination. The obtained optical parameters of gold were later used in the ellipsometric thickness measurements of the SAMs.

The synthesis of $HS(CH_2)_{15}CONH(CH_2CH_2O)_6H$ is described by Svedhem et al. [18]. The PEG750 compound (i.e., $HS(CH_2)_2CONH(CH_2CH_2O)_nCH_3$ compound with $n \approx 15$) was purchased from RAPP Polymere GmbH, Tübingen, Germany, and used as received. The OEG-SAMs were prepared by soaking the freshly cleaned gold substrates into 20 μM solutions for at least 48 h. The samples were then rinsed and ultrasonicated in ethanol for about 3 min, blown dry in nitrogen gas and immediately analyzed. The formation of SAMs of PEG750 was studied by contact angle goniometry (probing with fresh MilliQ water using Ramé–Hart NRL 100 goniometer) and null ellipsometry (assuming a three-zone model with an isotropic, transparent organic layer, $n = 1.5$) in air. The thickness d of the SAM was 51.6 ± 0.8 Å (error at 95% confidence level), and the advancing (θ_a) and rescinding (θ_r) contact angles were $48 \pm 2°$ and $44 \pm 2°$ (maximum errors), respectively. The observed thickness is in agreement with the theoretically calculated value of 49.8 Å. It should be stressed, however, that the contact angles of the SAMs formed using this commercial product are lower than those reported for shorter OEG-SAMs (cf. Harder et al. [8]). This lowering is attributed to a disordering of the outermost portion of the $HS(CH_2)_2CONH(CH_2CH_2O)_nCH_3$ SAM, most likely because of the distribution in chain length n. The corresponding thickness and contact angle values for the SAM formed by $HS(CH_2)_{15}CONH(CH_2CH_2O)_6H$ are known from our previous studies: $d = 39.8 \pm 1.7$ Å, $\theta_a = 28 \pm 2°$, $\theta_r = 25 \pm 2°$ [11c].

3. Results and discussion

3.1. Optimized geometries and helical parameters of ethylene glycol

The values of optimized bond lengths, bond angles, and dihedral angles for the $H(CH_2CH_2O)_6H$ molecule, henceforth referred to as EG_6, are compared in Table 1 with the internal coordinates for poly(ethylene glycol) (PEG) [12c]. Relatively small variations in optimized geometries were observed between the various methods of calculation. For instance, the difference in internal coordinates obtained by LSDA and B3LYP methods with the 3-21G* and 6-31G** basis sets does not exceed 3% for bond lengths, 2% for bond angles and 7% for dihedral angles.

Table 1
Internal coordinates (bond lengths, bond and dihedral angles) of PEG and the central C–C–O groups in the optimized structure of EG_6 with an indication of the method used in the calculations

Method	r(C–C) (Å)	r(C–O) (Å)	∠(COC) (°)	∠(CCO) (°)	τ(COCC) (°)	τ(OCCO) (°)
PEG[a]	1.54	1.43	111	111	191.5	60
DFT(LSDA)/3-21*	1.50	1.435	111	107	183	76
DFT(LSDA)/6-31**	1.50	1.40	112	109	184	72
B3LYP/3-21*	1.52	1.455	112.5	107	183	77
B3LYP/6-31**	1.51	1.41	113	109	183	72
RHF/6-31**	1.51	1.39	114.5	109	185	72
MP2/6-31**//HF/6-31**	1.51	1.42	112	108	184	71

[a] Data from Ref. [12c].

The atomic coordinates at the molecule equilibrium geometry have been used to find specific helical parameters of the ethylene-glycol chain [12a]. The results of the analysis for the EG_6 oligomer are summarized in Table 2, where the helical parameters calculated at the ab initio level are compared with the corresponding parameters calculated in [12c] for the theoretical model of helical PEG. Our notations are the same as in the quoted paper: θ is an angle of rotation about the helix axis on passing from one oxygen to another oxygen in the neighboring repeating unit; ρ(O) and ρ(C) are the distances from the chain atoms O and C to the helix axis, respectively; d(C–O) and d(C–C) are, respectively, the projections of the bonds onto the helix axis; θ(C–O) and θ(C–C) are the angles of rotation on passing from an atom to the adjacent atom.

In these calculations, the helical structure is deduced from the Cartesian coordinates of the central C–C–O groups. Since the EG_6 oligomer is too short to model even one period of the PEG (which requires approximately seven monomers), the identity of the oligomer and polymer helical structures may be questioned. We have checked therefore the fulfillment of the relations between the optimized internal molecular coordinates and the helical parameters θ, ρ(O), ρ(C), d(C–O), d(C–C), θ(C–O), and θ(C–C), which must be satisfied for an infinite helical chain [12b]. The

Table 2
Helical parameters of PEG and their counterparts in the EG_6 oligomer

Method	θ (°)	ρ(O) (Å)	ρ(C) (Å)	d(C–O) (Å)	d(C–C) (Å)	θ(C–O) (°)	θ(C–C) (°)
PEG[a]	102.9	0.56	1.6	0.83	1.09	31.5	40
DFT(LSDA)/3-21*	109.0	0.44	1.46	0.91	0.97	31.2	46.6
	(108.5)	(0.43)	(1.45)	(0.92)	(0.97)	(30.9)	(46.7)
DFT(LSDA)/6-31**	103.2	0.53	1.51	0.89	0.97	29.4	44.4
	(103.7)	(0.52)	(1.50)	(0.88)	(0.98)	(29.7)	(44.3)
B3LYP/3-21*	114.6	0.42	1.47	0.95	0.99	31.2	52.3
	(110.0)	(0.44)	(1.46)	(0.94)	(0.97)	(31.4)	(47.2)
B3LYP/6-31**	104.0	0.55	1.53	0.90	0.98	29.6	44.9
	(104.2)	(0.55)	(1.53)	(0.90)	(0.97)	(29.8)	(44.7)
RHF/6-31**	106.6	0.54	1.50	0.89	0.98	30.7	45.3
	(106.7)	(0.54)	(1.50)	(0.89)	(0.97)	(30.7)	(45.2)
MP2/6-31**//	104.7	0.53	1.54	0.88	0.96	30.1	44.5
HF/6-31**	(104.8)	(0.53)	(1.53)	(0.88)	(0.96)	(30.2)	(44.3)

In the calculations, we used the internal and Cartesian coordinates for the central C–C–O groups in the optimized geometry. The values in brackets are obtained as is explained in the text.

[a] Data from Ref. [12c].

values given in Table 2 (in brackets) are obtained from the relations just mentioned with the use of optimized internal coordinates. The closeness of the two sets of helical parameters indicates that OEGs with six or more repeating units possess almost perfect helical structure.

From the data presented, one can conclude that the HF, LSDA and B3LYP methods yield essentially the same equilibrium geometry (though different in details) of the OEG helical conformation. The dependence of the characteristic vibrational frequencies and corresponding TDMs on the choice of the method is far more critical. Comparing the frequencies obtained with the three methods, the LSDA gives the best agreement with the experimental data. Moreover, under reasonable assumptions regarding the band broadening, the intensity distribution in the reference RA spectra (represented below) is also best reproduced by the LSDA/3-21G* method/basis set, which fortunately is reasonable in terms of required computational time. In the following we compare the experimental RA spectra with simulated spectra based on ab initio modeling using the DFT-LSDA/3-21G* method.

3.2. Infrared spectroscopy

Conformational information about OEGs can be obtained in two frequency regions of the infrared spectrum: in the fingerprint region (900–1400 cm^{-1}), where different in-plane bending, wagging, twisting, rocking, and skeletal vibrations of the OEG portion give significant contribution; and in the CH_2-stretching region (2800–3000 cm^{-1}) contributed by vibrational excitations of both the alkyl and OEG portions of the molecule.

3.2.1. Fingerprint region

In the fingerprint frequency region, the alkyl part of the molecule has minor effects on the RA spectrum such as small shift and broadening of the OEG characteristic bands, etc. It makes sense, therefore, to compare the simulated spectra of a single EG_6 molecule with the experimental RA spectra of SAMs formed by the self-assembly of $HS(CH_2)_{15}CONH(CH_2CH_2O)_6H$ and $HS(CH_2)_2CONH(CH_2CH_2O)_{15}CH_3$ molecules on gold. From hereon these SAMs are referred to as the EG_6-SAM and EG_{15}-SAM, respectively.

Fig. 1A shows the calculated isotropic spectrum I_{av} (averaged over x-, y- and z-directions of the TDMs) of a single EG_6 molecule in the helical conformation. Furthermore, the simulated anisotropic spectrum I_z for the same molecule, modeled with the helix axis aligned parallel to the surface normal, is shown in Fig. 1B. The spectra in Figs. 1A,B are obtained as the sum of Gaussian-shaped peaks with the same half width, 4.5 cm^{-1}. The calculated and experimental frequencies, assignments and TDMs are summarized in Table 3.

The simulated isotropic and anisotropic spectra of EG_6 are compared with the experimental RA spectra of EG_{15}-SAM and EG_6-SAM, respectively, Figs. 1C,D. For convenience, the intensity of the spectrum shown in Fig. 1C is multiplied by a factor of 0.25. Though, neither the frequencies nor the peak intensities were scaled to fit experimental data, the similarity of the calculated and observed spectra is obvious. Hence the method of calculation and the relatively small basis set used can be

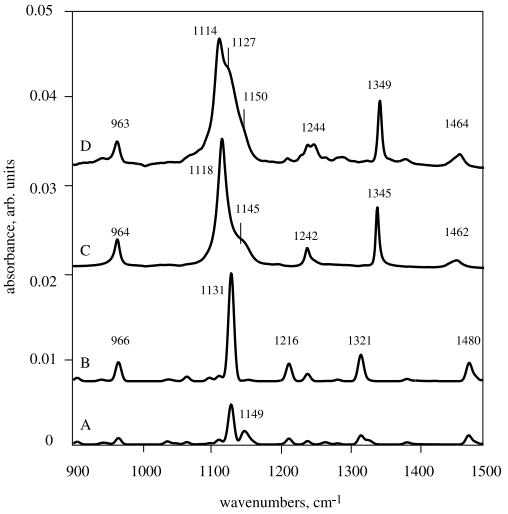

Fig. 1. Observed and calculated spectra in the fingerprint region. Curves D and C represent the RA spectra of the EG_6-SAM and EG_{15}-SAM, respectively. Curves A and B of EG_6 are calculated by DFT-LSDA method with 3-21G* basis set: curve B corresponds to the oligomer helix axis perpendicular to the SAM surface (I_z); curve A models the spectrum of randomly oriented EG_6 molecules (I_{av}).

Table 3
Frequencies (cm^{-1}), absolute values of TDMs (arb. units), and assignment of EG_6 dominant vibrational modes obtained by DFT-LSDA method with 3-21G* basis set; and frequencies of associated band maxima as they appear in the RA spectra of EG_6-SAM and EG_{15}-SAM

Calc. freq. EG_6	TDM[a]	Assignment of the calculated frequencies	Observ. freq.	
			EG_6-SAM	EG_{15}-SAM
Fingerprint region				
966	8.5 (z)	Asym. COC stretching + CH_2 rocking	963	964
1131	20.1 (z)	Asym. COC stretching	1114	1118
			~1127	
1149	8.8 (x), 6.1 (y)	Asym. COC stretching	~1150	~1145
1216	7.0 (z)	CH_2 twisting	1244	1242
1321	10.0 (z)	CH_2 wagging	1349	1345
1480	7.8 (z)	CH_2 scissoring	1464[b]	1462
CH_2-stretching region				
2866	3.9 (x), 3.4 (z)	Sym. stretching		
2886	10.3 (x), 2.3 (z)	Sym. stretching		
2889	12.0 (y)	Sym. stretching	~2864	~2864
2895	5.7 (y), 4.5 (z)	Asym. stretching		
2913	9.7 (x)	Asym. stretching		
2915	9.6 (y)	Asym. stretching		
2925	13.5 (z)	Asym. stretching	~2892	~2892

[a] Helix axis is parallel to z axis.
[b] This band is contributed by CH_2-scissoring modes from the alkyl and OEG chains.

regarded as appropriate for modeling the main features of the experimental spectra. The maximum deviation between calculated and experimental spectra is within ~2%. It is also evident that the modes with TDMs in the z-direction completely dominate the experimental spectra. Thus, a parallel orientation of the helix axis with respect to the surface normal appears to be a reasonable first-order approximation of the OEG-tail orientation within the SAM.

The experimental RA spectra also contain a few features that are not fully reproduced by our calculations. For example, the main peak near 1114 cm^{-1} has an asymmetric form, and the asymmetry is very prominent in the spectrum of the short oligomer EG_6-SAM, Fig. 1D. Previous studies suggest that amorphous and all-*trans* OEGs are expected to absorb in the 1125–1150 cm^{-1} region [8,11,12,19], and the shoulder(s) on the high frequency side therefore have been attributed to the presence of non-helical conformational states in the OEG-SAMs. Another possible explanation to the appearance of a high energy shoulder on the main peak is that the orientation of the helix axis deviates from being perfectly parallel to the surface normal, making contributions from vibrational modes with TDMs in the x, y-directions visible in the experimental RA spectra (a tilt of the helix axis can also be used to explain some of the differences seen in the CH_2-stretching region, Fig. 2, see discussion below).

We also carried out a sequence of calculations for a single EG_n molecule in the helical conformation for $n = 4, 5, 7$. The spectra obtained for these oligomers have similar shape and nearly linear increase in intensity (this result is also valid for the CH_2-stretching region). The fact that the overall form of the calculated spectra for OEGs of different lengths is very similar can be considered as an additional proof of the reliability of the computational procedure used.

3.2.2. CH_2-stretching region

The observed RA spectra of SAMs formed by OEG-terminated alkanethiolates are in the 2800–3000 cm^{-1} region due to vibrational motion of the alkyl and OEG parts of the molecules. Ideally, the calculated spectra of EG_6 should be compared

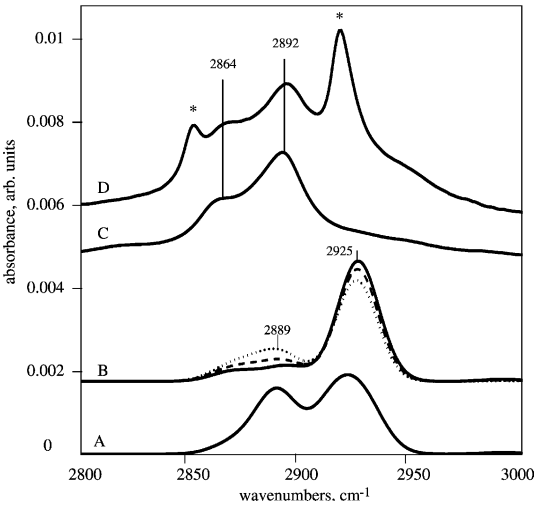

Fig. 2. Observed and calculated spectra in the CH_2-stretching region. Asterisks mark the absorption peak maxima at 2851 and 2918 cm^{-1} assigned to the symmetric and asymmetric CH_2-stretching modes of the alkyl chain [11]. The dashed and dotted lines correspond to the helix axis tilted by, respectively, 10° and 20° relatively to the surface normal.

with the data obtained for self-assemblies of OEG-terminated alkanethiolates with as short alkyl parts as possible. That is why we compare the calculated spectra of EG_6 molecule with the experimental spectrum of EG_{15}-SAMs that demonstrate excellent helical properties.

It is known [20] that the TDMs of CH_2-stretching modes are a superposition (with the corresponding phase shifts) of the dipole derivatives associated with each CH_2 group. The vector of dipole derivatives of the symmetric vibrations of the CH_2 group is directed along the bisector of the H–C–H angle, while the vector of the dipole derivatives of the asymmetric vibrations also lies in the H–C–H plane but it is perpendicular to the bisector of the H–C–H angle [21]. By using the ab initio optimized geometry obtained for EG_6, we calculated the angles between the bisectors of all CH_2 groups and the helix axis. It turned out that all these angles are very close to 90° (more precisely, their variation is within 7° between 87° and 94°). This means that the TDMs of the symmetric vibrations are oriented primarily perpendicular to the helix axis. Thus, the projection of the TDMs of the symmetric modes onto the helix axis should be rather small. In contrast, the asymmetric vibrations have TDMs of mixed character, see Table 3. It should be emphasized, however, that the most intense asymmetric mode has only a parallel (z) TDM component. Therefore, if the EG_n molecules are preferentially oriented along the normal to the surface, then the asymmetric vibrations will contribute significantly to the observed RA spectrum, while the symmetric peak must be very weak.

Table 3 represents the frequencies, the TDMs and assignments of the most prominent CH_2-stretching modes. The two strong modes near 2925 and 2889 cm^{-1} are identified as asymmetric and symmetric, respectively. The corresponding peak maxima can be found near 2892 and 2864 cm^{-1}, respectively, in the experimental RA spectra, Figs. 2C,D. Most importantly, our ab initio calculations clearly indicate that the dominating peak in the CH_2-stretching region (at 2892 cm^{-1}) originates from asymmetric vibrational modes. This assignment disagrees with that given in the work of Miyazawa et al. [12c], where the main peak was attributed to the symmetric mode. It should be pointed out, however, that Miyazawa and coworkers in fact admitted the controversy about assigning the main peak in the CH_2-stretching region to the symmetric mode, see for details the original paper [12c].

Fig. 2A displays the calculated isotropic spectrum I_{av}, while Fig. 2B shows the anisotropic spectrum I_z (solid line) in the CH_2-stretching region. The method of calculation and other details are the same as in the modeling of the fingerprint region with the only difference that the spectra are modeled with the use of a larger half-width value (9 cm^{-1}). If one compares the intensity distribution between the two main peaks at 2892 and 2864 cm^{-1} in the experimental RA spectra, Figs. 2C,D, with those in the simulated spectrum, Fig. 2B (solid line) then it becomes obvious that it is not possible to fit the data to a perfectly parallel orientation of the helix axis with respect to the surface normal. A tilt of the helix axis with 10° and 20° improves the fit (dashed and dotted lines, Fig. 2B) suggesting that a tilted orientation of the helix axis is likely. A tilted orientation is also consistent with the appearance of the x, y-mode near 1145 cm^{-1} as a high frequency shoulder on the main

peak in the fingerprint region, Figs. 1C,D. A more detailed analysis of the molecular orientation and phase behaviour of OEG-SAMs in the amorphous, all-*trans* and helical conformations will be addressed in subsequent publications.

4. Conclusion

The RA spectra of the monolayer self-assemblies of OEG-terminated alkanethiols on gold are discussed with a reference to ab initio modeling. The spectral features characteristic for the OEG portion in these SAMs have been compared with those of the calculated spectra, which were obtained by DFT and HF methods for $H(CH_2CH_2O)_nH$ oligomers in the optimized helical conformation. We have found that the most important spectral bands attributed to ethyleneglycol portion in the observed spectra can easily be recognized in the spectral curves simulated by the DFT-LSDA method. The calculated frequencies agree well with the experimental ones within approximately 2% (maximum deviation) without scaling. This result does not conclusively show that the OEG structure found here is the only one present in real SAMs, but it does support the fact that the present first-principle approach can be used as a platform to improve the understanding of RA spectra of organized molecular assemblies. It is probably even more important that the used DFT modeling approach can be expanded to include intermolecular interactions, in particular lateral hydrogen bond interactions in amide linked OEG-terminated alkanethiolates. These are our next target. Neither this possibility nor the close resemblance between the single-molecule and respective SAM spectra was obvious before our work. Now we are fairly confident that in addition to its own undoubted heuristic value, the ab initio single-molecule approximation also provides a firm basis for future studies (e.g., by molecular dynamics and/or Monte-Carlo methods) of the influence of intermolecular-interaction on the OEG-SAM structure and dynamics.

The above analysis of the peaks in the CH_2-stretching region has led us to the conclusion that the main peak near 2890 cm^{-1}, previously assigned to the symmetric stretching mode, originates in fact from intense asymmetric modes. This result is essential for the correct understanding of experimental data obtained by RA methods. At the same time, a number of other observations made on the basis of these calculations cannot be regarded as completely conclusive (at the level of single-molecule approximation) without establishing the relationship between the RA spectrum of the EG_n-SAM and the spectrum of its molecular constituents in their actual position within the SAM. Ab initio modeling of compounds with the general structure $HS(CH_2)_mXEG_nY$ in such a context will be addressed in forthcoming publications.

Acknowledgements

This work was supported by the Royal Swedish Academy of Sciences (for L.M. and Yu.K.) and the Foundation for Strategic Research (SSF) through the Biomimetic Materials Science program (for R.V. and B.L.). Computational resources were provided by the Swedish National Allocation Committee for High Performance Computing (SNAC). L.M. is grateful to S. Öberg for valuable discussions of practical aspects of the DFT method.

References

[1] P.E. Laibinis, J.J. Hickman, M.S. Wrighton, G.M. Whitesides, Science 245 (1989) 845;
K.L. Prime, G.M. Whitesides, Science 252 (1991) 1164.
[2] A. Ulman, Chem. Rev. 96 (1996) 1533.
[3] R.G. Nuzzo, D.L. Allara, J. Am. Chem. Soc. 105 (1983) 4481.
[4] P.E. Laibinis, G.M. Whitesides, D.L. Allara, Y.-T. Tao, A.N. Parikh, R.G. Nuzzo, J. Am. Chem. Soc. 113 (1991) 7152.
[5] M.A. Reed, C. Zhou, C.J. Muller, T.P. Burgin, J.M. Tour, Science 278 (1997) 252.
[6] J. Lahiri, L. Isaacs, J. Tien, G.M. Whitesides, Anal. Chem. 71 (1999) 777.
[7] C. Pale-Grosdemange, E.S. Simon, K.L. Prime, G.M. Whitesides, J. Am. Chem. Soc. 113 (1991) 12.
[8] P. Harder, M. Grunze, R. Dahint, G.M. Whitesides, P.E. Laibinis, J. Phys. Chem. 102 (1998) 426.
[9] A.J. Pertsin, M. Grunze, I.A. Garbuzova, J. Phys. Chem. 102 (1998) 4918.

[10] D.J. Vanderah, C.W. Meuse, V. Silin, A.L. Plant, Langmuir 14 (1998) 6916.
[11] (a) R. Valiokas, S. Svedhem, S.C.T. Svensson, B. Liedberg, Langmuir 15 (1999) 3390;
(b) R. Valiokas, M. Östblom, S. Svedhem, S.C.T. Svensson, B. Liedberg, J. Phys. Chem. B 104 (2000) 7565;
(c) R. Valiokas, M. Östblom, S. Svedhem, S.C.T. Svensson, B. Liedberg, J. Phys. Chem. B 105 (2001) 5459.
[12] (a) T. Miyazawa, J. Chem. Phys. 35 (1961) 693;
(b) T. Miyazawa, J. Polymer Sci. 55 (1961) 215;
(c) T. Miyazawa, K. Fukushima, Y. Ideguchi, J. Chem. Phys. 37 (1962) 2764.
[13] E.B. Wilson Jr., J.C. Decius, P.C. Cross, Molecular Vibrations, McGraw-Hill, New York, 1955.
[14] R.G. Snyder, G. Zerbi, Spectrochim. Acta 23A (1967) 391.
[15] S.P. Gejji, J. Tegenfeldt, J. Lindgren, Chem. Phys. Lett. 226 (1994) 427.
[16] R.L. Jaffee, G.D. Smith, D.Y. Yoon, J. Phys. Chem. 97 (1993) 12745.
[17] R.L.C. Wang, H.J. Kreuzer, M. Grunze, Phys. Chem. Chem. Phys. 2 (2000) 3613.
[18] S. Svedhem, S.-Å. Hollander, J. Shi, P. Konradsson, B. Liedberg, S.C.T. Svensson, J. Org. Chem. 66 (2001) 4494.
[19] D.J. Vanderah, G. Valincius, C.W. Meuse, Langmuir 18 (2002) 4674.
[20] P.C. Painter, M.M. Coleman, J.L. Koenig, The Theory of Vibrational Spectroscopy and its Application to Polymeric Materials, Wiley, New York, 1982.
[21] R. Zbinden, Infrared Spectroscopy of High Polymers, Academic Press, New York and London, 1964.